Plasma Modification of Cellulose Fibers for Composite Materials

J. Morales,[1] M. G. Olayo,[2] G. J. Cruz,[2] P. Herrera-Franco,[3] R. Olayo[1]

[1]*Departamento de Física, Universidad Autónoma Metropolitana, Unidad Iztapalapa, Apdo. Postal 55–534, Iztapalapa, D.F., 09340, México*
[2]*Departamento de Síntesis y Caracterización, Instituto Nacional de Investigaciones Nucleares, Apdo. Postal 18–1027, Col. Escandón, D.F., 11801, México*
[3]*Unidad de Materiales, Centro de Investigación Científica de Yucatán. Calle 43 # 130, Col. Chuburná, Mérida, Yucatán, México*

Received 26 May 2005; accepted 29 November 2005
DOI 10.1002/app.24085
Published online in Wiley InterScience (www.interscience.wiley.com).

ABSTRACT: Composites of natural fibers and thermoplastics can be combined to form new enhanced materials. One of the problems involved in this type of composites is the formation of chemical bonds between the fibers and the polymers at the interface. This work presents a study where low energy glow discharge plasmas are used to functionalize cellulose fibers implanting polystyrene between the fibers and the matrix that improve the adhesion of both components. The interface of polystyrene was synthesized by continuous and periodic glow discharges on the surface of the cellulose fibers. The results show that the adhesion in the fiber–matrix interface increases with time in the first 4 min of treatment. However, at longer plasma exposures, the fiber may be degraded reducing the adhesion with the matrix. © 2006 Wiley Periodicals, Inc. J Appl Polym Sci 101: 3821–3828, 2006

Key words: plasma polymerization; cellulose fibers; composites; styrene

INTRODUCTION

Polymeric materials reinforced with natural fibers have many potential industrial applications because the composite usually have better mechanical properties, as higher elastic modulus, higher strength, and lower density than the nonreinforced polymers. For example, density is a very important factor in mobile pieces in the transportation industry, where a weight reduction, without losing mechanical performance, means energy saving.[1,2] Depending on the kind of materials involved, the reinforced composites can also improve their resistance to corrosion, to wear, their appearance, stability, thermal conductivity, and both thermal and acoustic isolation.

Composite materials are constituted by more than one phase. One of them is usually stronger and is called reinforcement, and the other is a continuous phase, less rigid and weak called matrix. Because of chemical interactions or by effects of the processing, an additional phase can be generated at the interface between the reinforcement and the matrix.[3] The structure and properties of the interface play a very important role on the physical and mechanical properties of the composites due to the stress transfer between the matrix and the fibers. In turn, the adhesive properties of the interface are also influenced by the chemical and morphological compatibility of the two constituents.[4]

Composite materials with a weak interface have low tensile strength and a low rigidity, but on the other hand, they possess a greater strength to fracture. Materials with strong interfaces have a high tensile strength and a high rigidity, but they are fragile. The interface is also an important factor in the tenacity and fracture properties in wet and corrosive environments. Its importance is based in the adhesion between the fibers and the matrix, which depends on the superficial composition and on the topographic nature of the fiber.

The methods to modify the surface and to improve the mechanical operation of the fibers are different according to the type of matrix. The most common treatments modify the fibers by removing the superficial layer, changing the topography and the chemical nature of the surface. Organic fibers generally have smooth surfaces and little superficial energy, which result in low adherence to the matrix. These fibers usually do not have chemical functional groups to form covalent bonds in the fiber–matrix interface. In other works, the fibers have been treated superficially

Correspondence to: J. Morales (jmor@xanum.uam.mx).
Contract grant sponsor: CONACYT-México; contract grant number: I39261-U.

to increase the interfacial adhesion in environments where humidity is high and temperature is between 20 and 60°C.[5,6]

One less common technique to form chemical bonds and consequently to improve the adhesion in the fiber–matrix interface is the treatment by low-temperature plasmas.[7–10] It has been recognized that plasma treatments change the superficial properties of the material based on the formation of free radicals on the surface as a result of the impacts with the energetic particles (electrons, ions, etc) traveling in the plasma, or by photodecomposition of the surface carried out by the ultraviolet light generated by the plasma.

Glow discharges are efficient in creating a high density of free radicals in the gaseous phase and on the surface of the material being exposed to, including the most stable polymers. The superficial free radicals created by the plasma can react with each other or with other components activated in the plasma environment to form different chemical compounds.[11–13] They also increase the superficial energy of the fibers and modify the wet ability of the surfaces exposed to the plasma.[14–17]

Another possibility that can be added to the interface using plasmas is the simultaneous polymerization of monomers compatible to the fiber and to the matrix. The film formed in this way should have good adhesion to the fibers and to the matrix, but it should not alter the global properties of the fibers, because it solely modifies the surface.[18,19]

Thus, the surfaces of the fibers treated with plasma can result in stronger bonds with the matrices. For example, Kevlar fibers treated with argon and oxygen plasmas combined with polycarbonate increased the interfacial adhesion in 20 and 18%, respectively. Increases of the interfacial strain of 118% for Spectra fibers and of 45% for Kevlar fibers combined with the same epoxy resin have also been reported.[20]

In this way, the plasma treatment has four important effects on the organic substrates: cleaning, ablation, polymerization, and crosslinking. These four effects occur during the glow discharges and depend on the processing conditions such as reactor design, gas flow, operation voltage, power, pressure, temperature, etc. One or more of these effects can be dominant for a set of parameters of the glow discharges. However, in all cases, these processes only affect some of the external molecular layers.

In this work, polystyrene films were synthesized by plasma (PPS) on the surface of cellulose fibers to obtain a good compatibility between the fibers and a polystyrene (PS) matrix. The fundamental hypothesis of the plasma treatment is that the free radicals generated on the surface of the reinforcement fibers can form bonds to the matrix through the fiber–matrix interface.[18] The polystyrene interface was characterized by X-ray diffraction, FTIR, scanning electron microscopy, and thermogravimetric analysis. The microbond technique was used to study the effect of the plasma treatment on the fiber–matrix interface. Micromechanical analysis was done to the fibers to study the modification of the Young modulus (E_f), deformation at rupture, and tensile strength because of the plasma treatment.

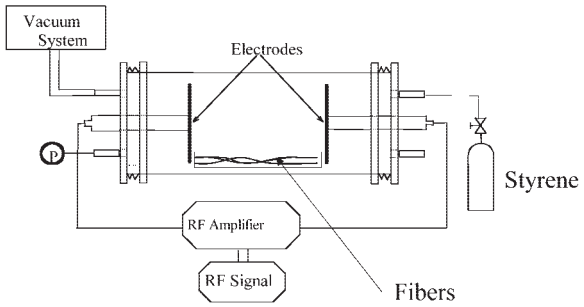

Figure 1 Experimental set up.

EXPERIMENTAL

The effect of the energetic particles in the plasma colliding with the fibers, breaking and forming superficial bonds with the monomer molecules, depends on the gas used and on the time of the plasma exposure.[18] The cellulose fibers in this work were exposed to the plasma within a polymerization reactor in which styrene reacts, polymerizes, and adheres to the surfaces. The monomer in vapor phase was introduced to the discharge chamber through one of the access ports (Fig. 1). The glow discharges were applied without carrier gas at a radio frequency operation of 13.5 MHz, temperature of 30°C, an average power of 12 W, and pressure of 4×10^{-2} Torr.[21–23]

Two kinds of plasma treatments were applied to the fibers: one with continuous and the other with periodic glow discharges. In the continuous discharge treatment, the plasma was active during 2, 4, and 6 min, samples Con-2, Con-4, and Con-6, respectively. In the periodic discharges, the plasma was on during 30 s followed by 10 min off. This procedure was repeated until completing 2, 4, 6, and 60 min of plasma treatment and samples Per-2, Per-4, Per-6, and Per-60, (4, 8, 12, and 120 cycles, respectively). At the end of both treatments, the fibers were left in a styrene atmosphere for 2 h.

The X-ray diffraction spectrum was obtained from the polymeric styrene films, with a SIEMENS D 5000 diffractometer scanned a 2θ angle between 5° and 35°. The FTIR spectra were taken with a FT-IR 2000 Perkin–Elmer spectrometer in a wavelength interval of 400–4000 cm^{-1}. The thermogravimetric analysis was made with a TA-Instruments analyzer using a heating ramp of 10°C/min from 20 to 650°C in a nitrogen

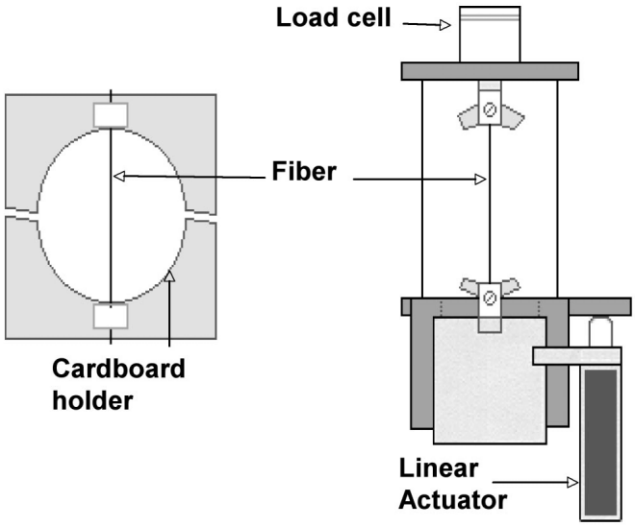

Figure 2 Schematic of the microtensile system used for the determination of the mechanical properties of the fiber.

atmosphere. The micro-mechanical tests were made on the fibers with a Minimat testing machine.

Materials and experimental procedures

Polystyrene (PS) in film-form from Aldrich was used as the matrix material. A T_g equal to 100°C and a degradation temperature of 425°C were measured for this material. Rayon fibers (Rayon yarn 1840, dtex f1000) from Akso Nobel were used as the reinforcing agent. The fiber diameter was measured by averaging ~50 readings taken by means of a calibrated eye-piece in an optical microscope (American Optical, model 120).

The mechanical properties of the fibers were obtained using a micro tensile system equipped with a 25 g load cell, a linear actuator (Newport, model PMC 200-P), and a translation speed of 0.02 mm/s (Figure 2). For testing, the fibers were affixed to a cardboard holder with circular cut-out using glue. Prior to testing, the holder sides were cut using scissors to let fiber free to support the applied load. The elongation of the fiber was registered recording the linear actuator displacement.

The fiber–matrix interfacial shear strength was measured using the microbond technique. The specimens were prepared as follows: A longitudinal cut was made in a small rectangular piece of film of the PS (about 4×1.5 mm^2) along nearly its entire length, to form two strips joined at one end for a distance of 50–100 μm. The strips had the appearance of a pair of trousers. Then, the strips were suspended on the horizontal fibers already affixed to a holding frame, and the thermoplastic was melted on the fibers. Upon melting, nearly uniform sized droplets were obtained.

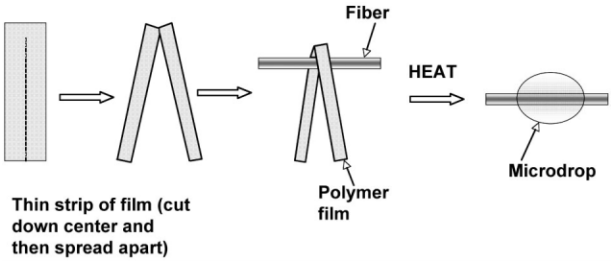

Figure 3 Schematic of the microdrop formation process.

Their diameters were controlled by the film length and thickness. This process is shown in Figure 3.

To pull the fiber out of the drop, the following experiment was performed: the droplets of polymer were kept in a fixed position using a pair of rectangular blades attached to a micrometer screw. The spacing between blades was kept constant to allow the fibers to pass in between them, while a steadily increasing force was applied to the free end of the fiber to pull it out from the drop. Load and displacement were monitored continuously using a 50 g load cell, until the fibers started sliding with respect to the matrix or until the fiber broke. In the last case, the experiment was not taken into account for the final calculations. This experimental set up was mounted on the stage of an optical microscope (American Optical, model 120). The strength of the average interfacial shear strength was calculated by dividing the maximum force of debond by the fiber embedded area as follows:

$$\tau = \frac{F_d}{\pi d L} \tag{1}$$

where τ is the average interfacial shear strength, F_d is the force at the moment of debonding, d is the fiber diameter, and L is the embedded fiber length.

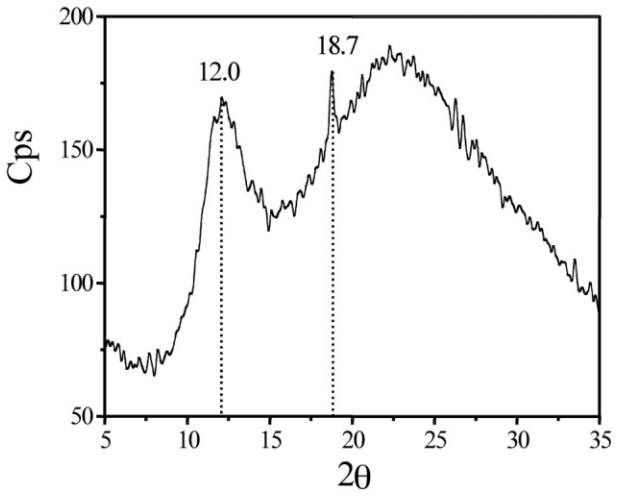

Figure 4 X-ray diffraction spectrum of polystyrene by plasma.

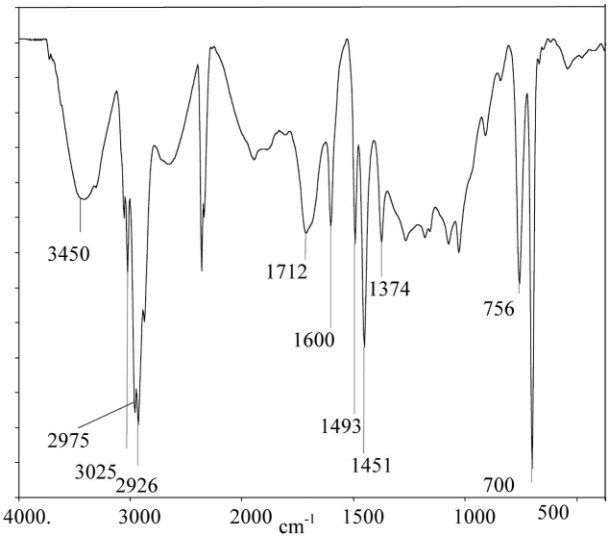

Figure 5 FTIR Spectrum of the polystyrene films synthesized by plasma.

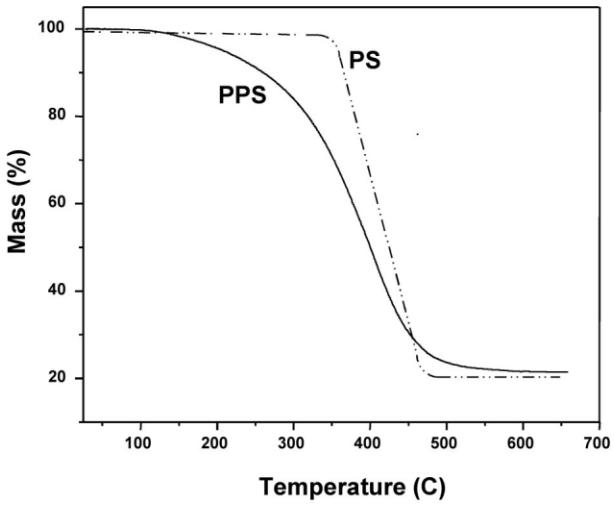

Figure 6 Thermal stability of polystyrene.

PPS characterization

Crystalline analysis

The traditional forms of PS synthesis produce an almost amorphous material; however, the plasma polystyrene has X-ray diffraction that suggests ordered segments in the polymers. Figure 4 presents the X-ray dispersion of PPS. Most of the dispersion corresponds to the amorphous content of the polymer; however, two crystalline peaks can be identified. The first one is located at $2\theta = 12.0°$ and the second one at $2\theta = 18.7°$. These two signals suggest that the chains of the polymer are accommodated in partially ordered regions, which can reach up to 19.6% of crystallinity. Both peaks have been identified, in approximately the same region, in the partially crystalline isotactic PS, although with different intensities.[24]

FTIR spectra

Figure 5 shows the FTIR spectrum of polystyrene films synthesized by plasma. The peaks in 756 and 700 cm^{-1} can be assigned to the out of the plane flexion of the phenyl ring. In 1451 cm^{-1} the absorption can be assigned to the flexion of the C—H methyl in the phenyl ring. The peaks at 1600 and 1493 cm^{-1} indicate the vibration of the phenyl ring.

In 2926 and 2975 cm^{-1} the vibration of the C—H groups is found. Centered in 3025 cm^{-1}, the vibration of the C—H aromatic groups is reported. The difference of intensities between the peaks of the aromatic C—H intensity in 3025 cm^{-1} and aliphatic C—H intensity in 2926 cm^{-1} can be used to indicate the aromaticity of the polymer. Therefore, calculating the aromaticity as $A = I_{3025}/(I_{3025} + I_{2926})$ from the Aldrich IR spectra of styrene and PS standards[25] and PPS, we have $A_{Sty} = 0.64$, $A_{PS} = 0.51$, and $A_{PPS} = 0.33$. A_{PPS} is approximately half of A_{Sty} and 35% lower than A_{PS}, which is an indication that the glow discharge, at those conditions, could break up to one third of the phenyl rings. This effect usually results in ramified and crosslinked structures in the plasma polymers. Crosslinked polymers bonding the fibers and the matrix should have a good adhesive function.

Centered in 1712 cm^{-1}, a complex absorption band corresponding to the C═O groups is found. This complex absorption is not found in the conventional polystyrene, and indicates the oxygen incorporation to the polymer. The absorption in 3450 cm^{-1} reinforces the hypothesis of the oxygen incorporation with the O—H vibration. The oxygen can be originated from two sources. As the reactor operates at 10^{-2} Torr, there are oxygen atoms still available to react with the styrene radicals and ions formed during the glow discharges. The second source of oxygen is originated from the ambient. When the polymerization reaction ends, the

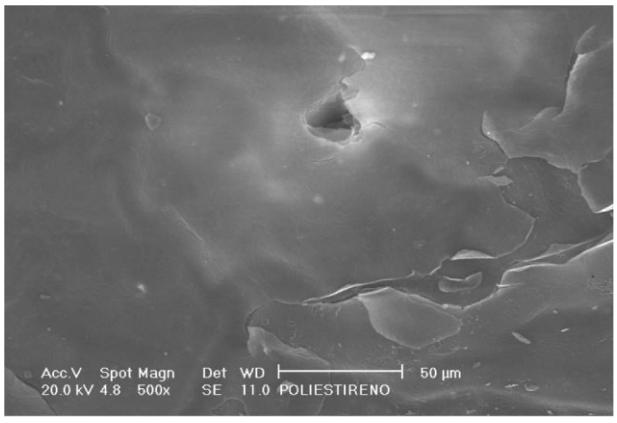

Figure 7 Layers of PPS.

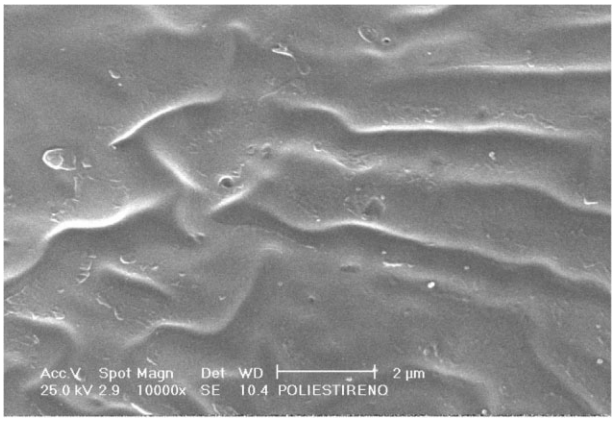

Figure 8 Surface of PPS films.

reactor is opened to the environmental conditions, and the radicals, which are still active on the polymer surface, react with the atmospheric oxygen.

Thermogravimetric analysis

Figure 6 presents a thermogravimetric analysis of PS and PPS. The polymers practically do not present absorption of humidity or any of the solvents used to separate the films from the substrate. In PS, a flat region without mass loss is found until 330°C. After this temperature, the polymers suffer a pronounced loss of mass that represents ~80% of its initial mass. This loss ends at ~470°C, and after this point, only fragments of the polymer chains remain in the heating zone.

In comparison with the thermal decomposition of PS, PPS has smaller thermal stability, beginning to decompose at ~130°C. After this point, the polymer has the main fall of mass until ~550°C, where it loses 75% of its initial mass. The trend of PPS decomposition is an indication of chains with different size or crosslinked structures.

Morphological analysis

Micrographs of PPS films are shown in Figures 7 and 8. The polymers have a layered growing pattern, accommodated in a non-continuous way with different depth levels between the layers. This type of growth is characteristic of the polymers formed by glow discharge plasmas. In Figure 8, the microscopic aspect of the film presents a smooth surface with long protuberances. These probably result from the solvents used to separate the film from the substrate.

Cellulose fibers characterization

Fiber diameter

The plasma treatment has two competitive effects, it etchs the fiber and synthesizes polymers at the surface; consequently, changes in the thermodynamic and electronic conditions during the process also induce small changes in one or in the other direction. To evaluate if the superficial plasma treatment modifies the dimensions of the fibers, a comparison of the fiber diameters after each treatment was carried out. The dimension measured correspond to the projection of the fiber diameter in a plane, the calculated average is known as the apparent diameter of the fiber and it was also used for the calculations of their mechanical properties and the interfacial shear strength. The results are shown in Table I. The small variation in the diameters reaches ~6 and 4% less in the continuous and periodic discharges, respectively. This variation is within the normal dispersion of the diameters in fibers with non-uniform transversal section. From a macro point of view, the results show that the two treatments do not change significantly the fiber diameter.

TABLE I
Apparent Diameter of the Cellulose Fibers

Cellulose fibers	Type	Diameter (μm)
Without treatment	A	12.2 ± 1.6
Continuous glow discharges		
2 min	Con-2	11.6 ± 0.7
4 min	Con-4	11.4 ± 0.6
6 min	Con-6	11.5 ± 0.7
Periodic glow discharges		
2 min	Per-2	11.6 ± 0.6
4 min	Per-4	12.2 ± 0.7
6 min	Per-6	11.9 ± 0.7
60 min	Per-60	11.9 ± 0.7

Tensile properties

Table II shows the results of the tensile strength and the elastic module of the fibers with the different

TABLE II
Mechanical Properties of the Untreated and Plasma-Treated Cellulose Fibers

Cellulose fibers	Treatment	Tensile strength (MPa)	Elastic modulus (GPa)
Without treatment	A	642 ± 109	8.7 ± 1.4
Continuous glow discharges			
2 min	Con-2	561 ± 80	11.4 ± 1.0
4 min	Con-4	667 ± 97	12.6 ± 1.5
6 min	Con-6	605 ± 54	10.7 ± 1.6
Periodic glow discharges			
2 min	Per-2	609±47	11.5 ± 0.8
4 min	Per-4	528 ± 96	10.8 ± 1.1
6 min	Per-6	662 ± 77	12.3 ± 1.1
60 min	Per-60	607 ± 82	11.5 ± 1.1

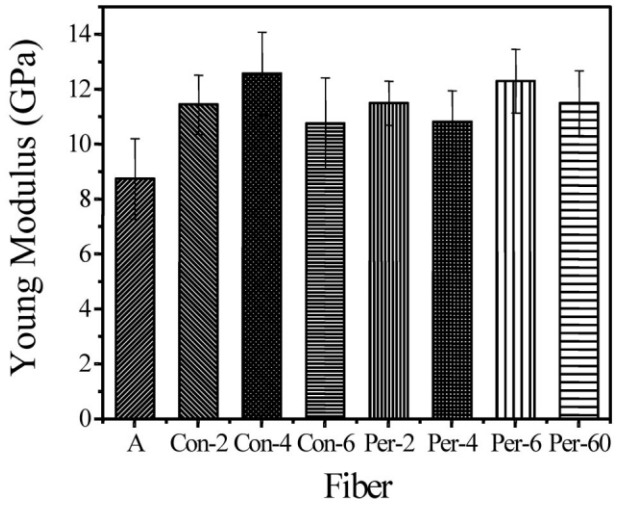

Figure 9 Elastic modulus as a function of fiber surface treatment.

treatments. The tensile strength of Con-4 and Per-6 fibers is ~4 and 3% higher, respectively, compared with the A fibers. In the case of the Per-4 fibers, the tensile strength is ~17% lower than that of the A fiber. It is noticeable that the superficial treatment has a detrimental effect on the tensile properties of the fibers.

During a plasma treatment, additionally to the formation of new bonds between the fibers and the polystyrene in progress, the continuous collisions of the plasma particles on the cellulose fibers may generate or propagate defects in the fibers that could lead to zones of probable ruptures.

Young modulus (elastic modulus)

The results shown in Table II indicate a tendency to increase the stiffness of the fibers with the plasma treatment. The increase ranges from 23% for the Con-6 fibers to 43% for the Con-4 fibers. Figure 9 illustrates the increase of the elastic module and shows the variation caused by the plasma treatments.

TABLE III
Average Interfacial Shear Strength

Cellulose fibers	Type	(MPa)
Without treatment	A	7.0 ± 2.0
Continuous glow discharge		
2 min	Con-2	10.6 ± 2.1
4 min	Con-4	9.9 ± 1.7
6 min	Con-6	9.1 ± 1.6
Periodic glow discharge		
2 min	Per-2	11.9 ± 2.4
4 min	Per-4	10.1 ± 2.5
6 min	Per-6	9.7 ± 2.1
60 min	Per-60	7.8 ± 1.5

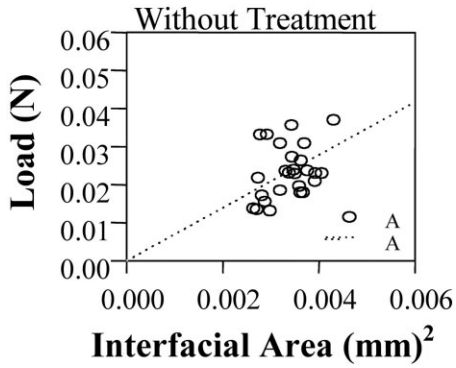

Figure 10 Fiber–matrix interfacial shear stress for fibers without plasma treatment.

Interfacial characterization

Table III shows the average strain interfacial obtained from microdrop tests for each plasma treatment applied to the fibers. Figures 10–12 plot the interfacial area versus their respective maximum load registered prior to failure in the interface, which is, prior to the separation of the fiber from the PS matrix. A linear behavior is observed because, if the interfacial area increases, the value of the load also increases. Because of the inherent data dispersion of the test, the slope of the best fitted line is considered as the average interfacial shear stress. This line will also be used to illustrate the variation of the average interfacial shear stress of the fibers after treatment with respect to that corresponding to fibers without any treatment.

Figure 10 shows the fiber–matrix interfacial shear stress without the plasma treatment. This behavior will serve as a reference to analyze the fiber interface submitted to superficial plasma treatment. To carry out a better interfacial strength analysis, the results of the continuous glow discharge and subsequently the

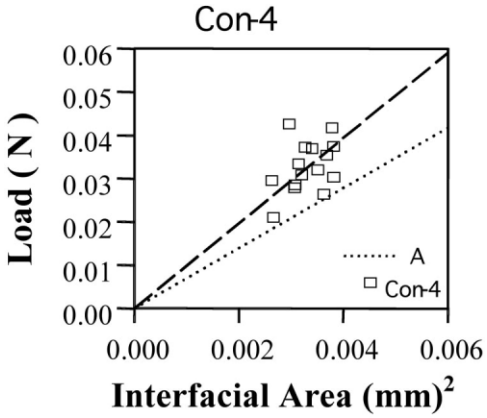

Figure 11 Fiber–matrix interfacial stress with continuous glow discharge treatments, exposure time of 4 min.

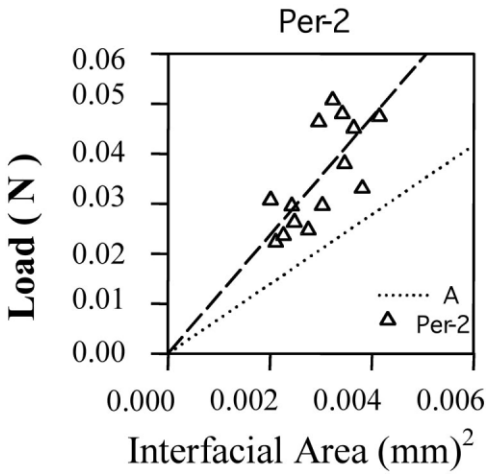

Figure 12 Fiber–matrix interfacial stress with periodic glow discharge treatments, exposure time of 2 min.

periodic glow discharge are discussed in the next sections.

Continuous glow discharges. The fibers with plasma treatment increased their interfacial strength, as is illustrated with the slope line adjusted to the experimental data in Figure 11. As the time of exposure increases, the interfacial strength is reduced with respect to the fibers without plasma treatment. This means that when the treatment time increases, the excited styrene molecules continue colliding with the fibers, thus continuing the breaking of bonds and forming new chemical bonds with them. The surface modification also increases, reaching the maximum adhesion strength in the interface at those conditions.

Periodic glow discharges. The results for this treatment show an increase in the interfacial resistance with respect to the fiber without treatment, as is illustrated in Figure 12. In a similar way, the interfacial resistance of the fibers treated with continuous glow discharges reduces as the time of exposure increases.

Figure 13 shows a comparison of the interfacial shear

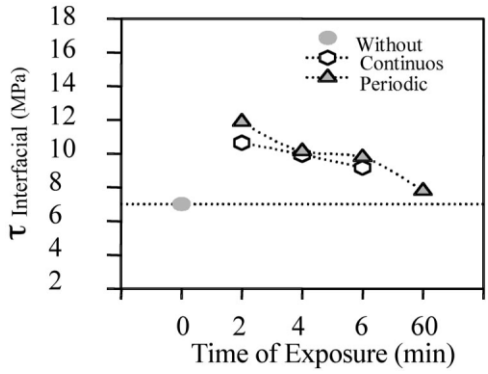

Figure 13 Interfacial shear strength as a function of time of exposure.

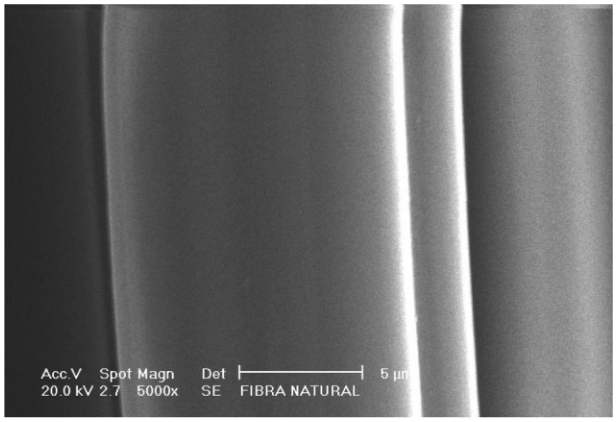

Figure 14 Fibers without treatment.

strength of the fibers treated with continuous and periodic plasma glow discharges at different exposure times. At the same exposure time, the fibers with periodic treatment present a greater increase in the interfacial shear strength compared with those fibers with continuous treatment. The time of exposure plays an important role in the modification of the surface.

The effective contact time of the excited styrene molecules on the fiber in pulsated glow discharges is less than in the continuous discharges causing that the surface of the fiber has fewer sites of possible interaction, but the constant styrene flow allows that the active sites result in polymeric chains strongly bonded to the fibers with an improvement in the interfacial strength.

The greatest increase in the interfacial strength was about 70% in the Per-2 fibers, with periodic glow treatment at the smallest time of exposure, 2 min. On the other hand, the Per-60 fibers with 1 h time of exposure of periodic glow discharges had the smallest increase, 18%, suggesting also that the interfacial resistance reduces as the time of exposure increases.

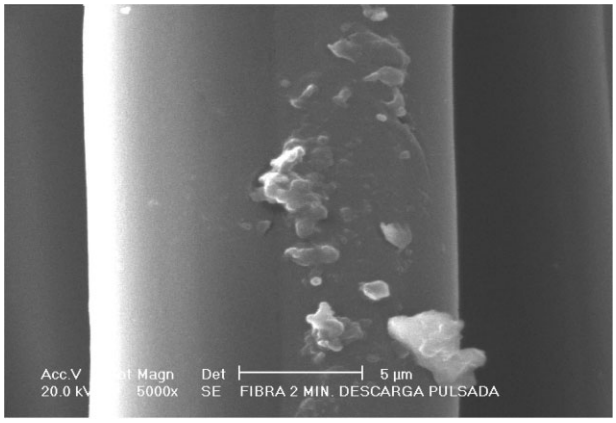

Figure 15 Periodic glow discharge 2 min, Per-2.

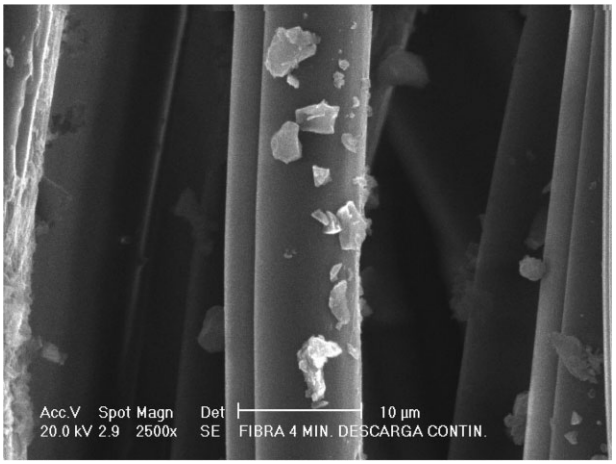

Figure 16 Continuous glow discharge, Con-4.

Morphology of the fibers

Figure 14 shows a micrograph of a cellulose fiber without treatment. The surface of the fiber is smooth and uniform. This type of morphology avoids that some other material easily adhere to the fiber causing a very weak interface. Figures 15 and 16 contain micrographs of fibers exposed to 2 min of periodic glow discharges and 4 min of continuous glow discharges, respectively.

In Figure 15, the photograph shows small fragments of polystyrene adhered to the fiber in several points. This is an indication that the periodic glow discharges create different activation sites that promote the formation of chemical bonds between the polymeric matrix and the fibers. It is important to note that the photograph does not show physical damage on the fiber.

Figure 16 shows fragments of polystyrene adhered on the fiber as a result of 4 min of a continuous glow discharge. The continuous discharges produce less polystyrene than the periodic glow discharges. Note the etched surface of the fibers in the left side of the micrograph due to the plasma treatment.

CONCLUSIONS

The polystyrene films obtained by plasma in this work, as the interface of the cellulose fibers and a polystyrene matrix, have ordered regions with crystallinity up to ~20%. However, the resulting polymer is a combination of chains with monomer molecules and fragments of them that is less thermally stable than the polystyrene synthesized by the traditional chemical methods. Such complex structures can include ramification and crosslinking at the interface, which increases the bonding between the fibers and the matrix. Thus, the adhesion in the fiber–matrix interface increases with the plasma treatment. Nevertheless, at longer time of exposures, the fiber may degrade due to the constant impact of particles on the surface and consequently, the adhesion in the fiber–matrix interface decreases. The main changes were obtained in the first 4 min of treatment, wherein the continuous and periodic discharges on the fibers increased the interfacial resistance respect to the fibers without treatment.

The authors acknowledge to CONACYT-México, project I39261-U, for the partial support to this work and Leticia Carapia from the ININ Laboratory of Electron Microscopy for her help with the SEM analysis.

References

1. Hull, D. In Materiales Compuestos; Editorial Reverté S. A., España: Barcelona, 1987; pp 1–58.
2. Isaac, M. D.; Shai, O. Engineering Mechanics of Composite Materials; Oxford University Press: New York, 1994; pp 3–31.
3. Kim, J.-K.; Mai, Y.-W., Eds. Engineered Interfaces in Fiber Reinforced Composites; Elsiever: Amsterdam, 1998; pp 171–186.
4. Mark, H. F.; Bikales, N.; Overberger, C. G.; Menges, G.; Kroschwitz, J. I. Encyclopedia of Polymer Science and Engineering, 2nd ed.; Wiley: New York, 1985; Vol. 1, pp 490–491.
5. Li, Z.-F.; Netravali, A. N. J Appl Polym Sci 1992, 44, 319.
6. Hochart, F.; De Jaeger, R.; Levalois-Grutmacher, J. Surf Coat Technol 2003, 165, 201.
7. Caro, J. C.; Lappan, U.; Simon, F.; Pleul, D.; Lukwitz, K. Eur Polym J 1999, 33, 1149.
8. Steen, M. L.; Flory, W. C.; Capps, N. E.; Fisher, E. R.Chem Mater 2001, 13, 2749.
9. Chen, M.; Yang, T. C.; Ma, S. G. J Polym Sci Part A: Polym Chem 1998, 96, 1265.
10. Denes, F. S.; Manolache, S. Prog Polym Sci 2004, 29, 815.
11. Hegemann, D.; Brunner, H.; Oehr, C. Plasma Polym 2002, 6, 221.
12. Cho, D. L.; Sjoblom, E. J Appl Polym Sci Appl Polym Symp 1990, 46, 461.
13. Barton, D.; Bradley, J. W.; Steele, D. A.; Short, R. D. J Phys Chem B 1999, 103, 4423.
14. Gil'man, A. B. High Energy Chem 2003, 37, 17.
15. Paterno, L. G.; Manolache, S.; Denes, F. Synth Met 2002, 130, 85.
16. Pitt, W. G.; Lakenan, J. E.; Strong, A. B. J Appl Polym Sci 1993, 48, 845.
17. Chen, J. R. J Appl Polym Sci 1991, 42, 2035.
18. Nay, J. C.; Pitt, W. G.; Armstrong-Carroll, E. J Appl Polym Sci 1995, 56, 461.
19. Biro, D. A.; Pleizer, G.; Deslandes, Y. J Appl Polym Sci 1993, 47, 883.
20. Piggott, M. R. Compos Sci Technol 1991, 42, 57.
21. Cruz, G. J.; Morales, J.; Castillo-Ortega, M. M.; Olayo, R. Synth Met 1997, 88, 213.
22. Cruz, G. J.; Morales, J.; Olayo, R. Thin Solid Films 1999, 342, 119.
23. Morales, J.; Olayo, M. G.; Cruz, G. J.; Castillo-Ortega, M. M.; Olayo, R. J Polym Sci Part B: Polym Phys 2000, 38, 3247.
24. Alexander, L. E. X-Ray diffraction methods in polymer science; Krieger: FL, 1979.
25. Pouchert, C. J., Ed. The Aldrich Library of FT-IR Spectra, 1st ed.; Sigma-Aldrich Co., USA 1998; Vol. 3.